

# Solution pH Alters Mechanical and Electrical Properties of Phosphatidylcholine Membranes: Relation between Interfacial Electrostatics, Intramembrane Potential, and Bending Elasticity

Yong Zhou\* and Robert M. Raphael<sup>†</sup>

\*Department of Biochemistry and Cell Biology, <sup>†</sup>Department of Bioengineering, Rice University, Houston, Texas

**ABSTRACT** Solution pH affects numerous biological processes and some biological membranes are exposed to extreme pH environments. We utilized micropipette aspiration of giant unilamellar vesicles composed of 1-stearoyl-2-oleoyl-phosphatidylcholine to characterize the effect of solution pH (2–9) on membrane mechanical properties. The elastic area compressibility modulus was unaffected between pH 3 and 9 but was reduced by ~30% at pH 2. Fluorescence experiments utilizing the phase-sensitive probe Laurdan confirmed gel-phase characteristics at pH 2, explaining the reduction of membrane elasticity. The membrane bending stiffness,  $k_c$ , increased by ~40% at pH 4 and pH 9 over the control value at pH 6.5. Electrophoretic mobility measurements indicate that these changes are qualitatively consistent with theoretical models that predict the effect of membrane surface charge density and Debye length on  $k_c$ , substantiating a coupling between the mechanical and interfacial electrical properties of the membrane. The effect of pH on intramembrane electrical properties was examined by studying the spectral shifts of the potentiometric probe di-8 ANEPSS. The intramembrane (dipole) potential ( $\Psi_d$ ) increased linearly as the solution pH decreased in a manner consistent with the partitioning of hydroxide ions into the membrane. However, changes in  $\Psi_d$  did not correlate with changes in  $k_c$ . These mechanical and electrical studies lead to the conclusion that the effect of pH on membrane bending stiffness results from alterations in interfacial, as opposed to intramembrane, electrostatics.

## INTRODUCTION

The solution pH affects many membrane-mediated biological processes, such as membrane fusion (1), cholesterol domain formation (2,3), drug-liposome interactions (4), membrane phase transitions (5–9), and erythrocyte deformability and spectrin solubility (10). Normally, extracellular fluids have a pH at ~7.4, and cells regulate their internal pH at ~7.0. However, in some situations biological membranes are exposed to environments with various pH values. For instance, the inner membranes of endosomes and lysosomes constantly face pH environments as low as 5 (11,12). In the mammalian stomach, apical membranes of gastric surface mucous cells and mucous neck cells, as well as canalicular membranes of parietal cells, constantly face a gastric juice whose pH varies from <1 to 6 (13). The phospholipid layer covering the gastric intestinal tract is also exposed to this corrosive gastric juice (14,15). The mechanism(s) that membranes of these cells and cellular organelles utilize to maintain integrity is still not well understood. Thus, characterizing and understanding the interactions between protons, hydroxide ions, and biomembranes is an important biophysical problem.

Proton-lipid interactions have been studied extensively using a variety of techniques such as EPR and NMR spectroscopy (16), Langmuir film balance (15,17–20), and fluorescence spectroscopy (21). These techniques have documented changes in many membrane properties in response

to changes in pH, including liposome stability, lateral phase separation, and the interdigitated gel-to-bilayer gel phase transition (15–21). In particular, calorimetric studies have established that low pH environments ( $\leq 2$ ) can increase lecithin membrane phase-transition temperatures (6–9,22,23). From the mechanical standpoint, the effect of pH on membrane interfacial tension has been studied by measuring the curvature change of a phosphatidylcholine (PC) lipid pendant drop exposed to different pH environments (22–26). The interfacial tension of PC lipids was observed to increase near pH 4 (25). However, to the best of our knowledge, the effect of pH on membrane mechanics and electrostatics has not been systematically studied in membrane vesicles. Thus, we were motivated to examine the effect of solution pH (2–9) on the mechanical and electrical properties of liposomal membranes to enable us to better understand the effect of protons and hydroxide ions on membrane stability. An additional outcome of this work is that alterations in solution pH provide a straightforward method to alter membrane electrostatics, and permit us to investigate the relationship between the mechanical and electrical properties of membranes and test theoretical models of these interrelationships.

Biomembranes are stabilized by the opposing forces of surface tension arising from hydrophobic forces and surface pressure resulting from repulsive interactions among lipid headgroups (27,28). Both surface tension and surface pressure are determined by inter- and intramolecular interactions of lipids, which define the cross-sectional area and the acyl-chain length of a given lipid molecule (29,30). For a collection of lipids that have self-assembled into a vesicle, a

*Submitted August 31, 2006, and accepted for publication November 20, 2006.*

Address reprint requests to R. M. Raphael, Tel.: 713-348-3494; E-mail: raphael@rice.edu.

© 2007 by the Biophysical Society

0006-3495/07/04/2451/12 \$2.00

doi: 10.1529/biophysj.106.096362

very small yet finite membrane tension exists that is defined as the difference between surface tension and surface pressure (31). The application of pressure to a vesicular membrane, experimentally realized in the micropipette aspiration method, changes the membrane surface area and can be used to determine the mechanical properties of the membrane. The bending stiffness,  $k_c$ , can be determined by measuring the tension required to smooth the membrane thermal undulations (32,33). As the membrane is further stretched by applied tension, actual changes in membrane surface area occur and are resisted by the elastic compressibility modulus,  $K_A$ . The method of micropipette aspiration has been effectively used to study the effect of ions and surfactant molecules on bilayer mechanical properties (32,34–40). For instance, salicylate, an active metabolite of aspirin predominantly anionic at neutral pH, decreases the bending stiffness and the apparent compressibility modulus of the membrane (34). Water-soluble bile acids, which are also mainly in anionic form at neutral pH, also partition into the membrane in a tension-dependent manner and reduce the apparent compressibility modulus (41).

When the membrane is exposed to ions, such as protons and hydroxide ions, inter- and intramolecular interactions, especially electrostatic interactions, can be altered. Zwitterionic PC lipid molecules contain functional groups (phosphate and choline), whose electric charge distribution at the membrane interface is a function of the binding of counterions (27,42–44), including protons and hydroxide ions. These interactions can potentially change interfacial electrical properties such as membrane surface charge density and  $\zeta$ -potential. The  $\zeta$ -potential,  $\zeta$ , which measures the potential slightly above the membrane interface and relates to the membrane surface charge density, is calculated from liposome mobility in an applied electric field (27). The interaction of ions with the membrane can also conceivably affect membrane mechanics, and there is experimental evidence that changes in ionic strength affect lipid packing (44,45). A number of theoretical models have predicted an intricate relationship between the mechanical and electrical properties of membranes (46–50). In particular, Winterhalter and Helfrich (46,47) developed models using Poisson-Boltzmann theory, which predict that changes in interfacial electric properties, such as the Debye length and membrane surface charge density, can affect the membrane bending stiffness. However, testing such models has proven experimentally difficult.

In addition to altering interfacial electrostatics, ions, including protons and hydroxide ions, can also potentially affect intramembrane electrostatics such as the dipole potential (51). The dipole potential,  $\Psi_d$ , arises from intrinsic internal dipole moments carried by both lipid functional groups and interfacial water molecules (27,52,53) and is crucial to many membrane-mediated biological processes (44,52–55). Membranes usually have a large ( $\sim 300$  mV) dipole potential that is positive inside of the bilayer core,

which is believed to be the main reason phospholipid bilayers are more permeable to anions than to cations (51–53). The dipole potential can be determined by measuring spectral shifts of the voltage-sensitive probe di-8 ANEPPS (51,53,56–58). Studies have established that the dipole potential is sensitive to lipid headgroup composition and external ions (51–53,56). The ability of ions to change the dipole potential correlates with the ion's free energy of hydration, following the Hofmeister series (51). It is not known whether there is a correlation between the dipole potential and the mechanical properties of the membrane.

In this study, we utilized micropipette aspiration of giant unilamellar lipid vesicles (GUVs) to investigate the interactions between the electrical and mechanical properties of membranes exposed to different pH environments. We found that the elastic compressibility modulus of SOPC membranes was reduced to 166 mN/m at pH 2, which we attribute to the appearance of gel-phase domains. The bending stiffness increased at pH 4 to  $1.2 \times 10^{-19}$  J and at pH 9 to  $1.3 \times 10^{-19}$  J. To determine whether these effects were related to changes in the interfacial and/or intramembrane electrical properties, we complemented the micromechanical measurements by determining the effect of pH on the  $\zeta$ -potential, as measured by the electrophoretic mobility of large unilamellar vesicles (LUVs) and on the dipole potential, as measured by spectral shifts in di-8 ANEPPS. The  $\zeta$ -potential data and measured changes in  $k_c$  are qualitatively consistent with the theoretical model of Winterhalter and Helfrich (46,47) and support the view that the effect of solution pH on  $k_c$  arises from contributions of both the membrane surface charge density and the Debye length. The pH effect on the membrane dipole potential is suggested to originate from the preferential interaction of hydroxide ions with the membrane. Thus, our  $k_c$ ,  $\zeta$ , and  $\Psi_d$  measurements indicate that the pH effect on PC membranes can be twofold. On one hand, protons and hydroxide ions can act as counterions and associate with phosphate and choline groups of PC lipids at the membrane interface. In addition, hydroxide ions affect the internal dipole potential of the membrane. While alterations in interfacial electrostatics correlate with changes in the bending stiffness, there does not appear to be a correlation between the intramembrane potential and the mechanical parameters. Taken together, the data support the view that intermolecular electrostatic interactions at the membrane interface can influence membrane mechanics and consequently affect the bending elasticity of bilayer.

## MATERIALS

The phospholipid 1-stearoyl-2-oleoyl-phosphatidyl-choline (SOPC) was purchased from Avanti Polar Lipids (Alabaster, AL). Lipids were dissolved in chloroform and stored at  $-20^\circ\text{C}$  under nitrogen. Fluorescent probes di-8 ANEPPS and Laurdan were purchased from Molecular Probes (Carlsbad, CA). Bovine serum albumin (BSA) was purchased from Sigma-Aldrich (St. Louis, MO). Glucose, sucrose, sodium hydroxide, and hydrochloric acid were purchased from Fisher (Pittsburgh, PA).

## METHODS

### Vesicle formation

Vesicles were formed from SOPC using a previously described electroformation procedure (34,59). Briefly,  $\sim 30 \mu\text{l}$  of 0.5 mg/ml SOPC/chloroform solution was spread on platinum electrodes in a Plexiglass chamber. The lipid film was then dried under vacuum for at least 2 h to completely evaporate chloroform. The chamber was filled with 200 mM sucrose solution and an alternating AC field of 0.5–2 V was applied to the electrodes at frequencies varying from 10 Hz to 1 Hz. After  $\sim 2$  h, the vesicles were harvested and stored at 4°C under nitrogen. We previously established that this protocol does not oxidize SOPC lipids (34). Thin layer chromatography has been performed to examine the effect of extremely acidic pH (pH 2) and alkaline pH (pH 9) on the chemical composition of PC lipids. No evidence of acid hydrolysis or saponification byproducts were found in SOPC lipids at the tested pH values (data not shown).

### Micropipette aspiration

Microaspiration measurements were performed on the stage of a Zeiss Axiovert 200M inverted microscope equipped with differential interference contrast optics and a Zeiss PLAN-NEOFLUAR 40 $\times$ /0.85 polarized differential interference contrast objective (Carl Zeiss, Thornwood, NY) at 1.6 optovar. Micropipettes were fabricated using a micropipette puller (Sutter P-97, Novato, CA) and then cut cleanly on a custom-made microforge. A 0.02% bovine serum albumin (BSA) solution was used to coat the pipette and coverslips. An extensive washing of the coated pipette and coverslips with both 200 mM glucose solution and distilled water was performed in an effort to eliminate excess BSA on the pipette and coverslips (34,35).

Pressure manipulation was achieved by coupling the micropipette in the chamber to a water-filled reservoir mounted on a motorized mechanical slider (Robocylinder, Torrance, CA) with resolution of 0.01 mm. The pressure level was calibrated and periodically checked using small vesicular debris ( $\sim 1$ – $2 \mu\text{m}$  in diameter) in the chamber. Giant unilamellar vesicles were added in the aspiration chamber filled with an isomolar glucose solution (200 mOsm) that was freshly prepared before each experiment and adjusted to the desired pH. Since this is a study of electrostatic effects of solution pH, specifically effects of protons and hydroxide ions, on membrane mechanics, the solutions were not buffered so that data interpretation would not be complicated by the presence of various ions in a buffer. The pH of the solutions used in experiments was periodically checked after experiments and the change in pH was  $<0.07$  pH units. The insertion of the glass micropipette was also found not to affect solution pH. A negative pressure was applied to create a vesicular projection which was given  $\sim 8$ – $10$  s to achieve steady state. Aspiration images were captured using a Zeiss AxioCam MRm camera and analyzed using Zeiss Axiovision 3.0 software. To ensure accuracy of the analysis, measurements were periodically checked using comparative light intensity plots of the corresponding vesicle images (34,60). All measurements were conducted at room temperature.

The membrane tension ( $\tau$ ) and apparent fractional area change ( $\alpha_{\text{app}}$ ) were obtained using (32,34,39)

$$\tau = \frac{(P_o - P_p)R_p}{2(1 - R_p/R_v)}, \quad (1)$$

$$\alpha_{\text{app}} = \frac{\Delta A}{A} = \frac{2\pi R_p \Delta L (1 - R_p/R_v)}{4\pi R_v^2 - \pi R_p^2 + 2\pi R_p L}, \quad (2)$$

where  $A$  is the total membrane surface area;  $\Delta A$  is the change in area resulting from applied tension;  $R_v$  and  $R_p$  are radii of the aspirated vesicle and pipette, respectively;  $L$  is the vesicle projection length; and  $\Delta L$  is the change in  $L$  resulting from the change in tension. The geometrically measured area expansion is designated as apparent area change. A plot of  $\tau$  versus  $\alpha_{\text{app}}$  reveals an initial exponential domain ( $\tau < 0.5$  mN/m) domi-

nated by thermally driven out-of-plane fluctuations of the membrane surface (61) that is followed by a region of linear elastic behavior ( $\tau > 0.5$  mN/m) whose slope is the apparent compressibility modulus,  $K_{\text{app}}$  (32,34,39) (Fig. 1 *a*). The bending modulus,  $k_c$ , is obtained from the slope of a plot of  $\ln(\tau)$  versus  $\alpha_{\text{app}}$  (Fig. 1 *b*) in the low-tension region, which is equal to  $8\pi k_c/k_B T$  (61).

### Elastic area compressibility modulus ( $K_A$ )

In the aspiration experiments, membrane thermal undulations occur throughout the entire tension range. This means that a portion of the measured area change at all tension levels is caused by smoothing of thermal undulations (61). This portion is calculated as

$$\Delta\alpha(i) = (k_B T / 8\pi k_c) \ln[\tau(i) / \tau(1)], \quad (3)$$

where  $\tau(1)$  is the initial tension. To obtain the elastic compressibility modulus ( $K_A$ ),  $\Delta\alpha(i)$  at each tension point  $i$  was removed from the measured total area ( $\alpha_{\text{app}}(i)$ ) using the models developed previously (32,61). Mathematically, the actual elastic area dilation, denoted  $\alpha_A$ , is calculated at each point as  $\alpha_A(i) = \alpha_{\text{app}}(i) - \Delta\alpha(i)$  (32,61). The elastic area compressibility modulus ( $K_A$ ) for each vesicle was calculated from the slope of data replotted as  $\tau$  versus  $\alpha_A$ .

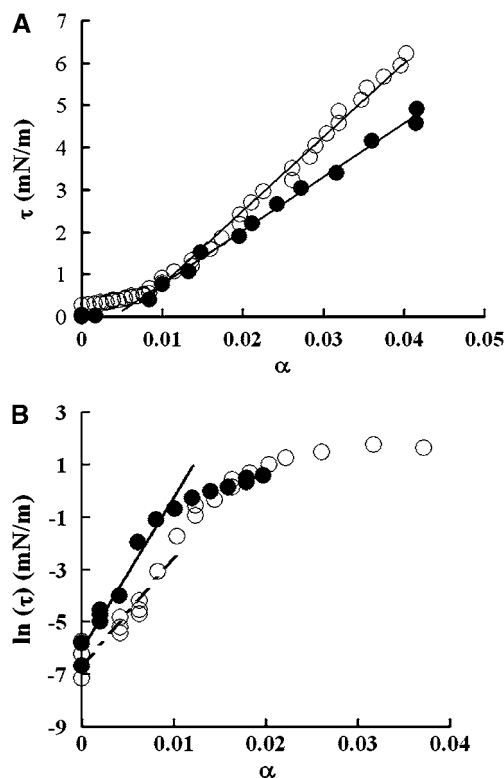


FIGURE 1 (*a*) Plots of tension ( $\tau$ ) versus fractional area change ( $\alpha$ ) for a representative vesicle in 200 mM glucose at pH 6.5 (○) and for another vesicle in solution at pH 2 (●). The slope of the high tension region ( $>0.5$  mN/m) is the apparent area compressibility modulus ( $K_{\text{app}}$ ). (*b*) Plots of  $\ln(\tau)$  versus  $\alpha$  for a control vesicle in 200 mM glucose at pH 6.5 (○) and another vesicle in solution at pH 4 (●), in which  $\alpha$  in the low tension region was carefully measured. The slope of the low-tension domain of the plot was used to calculate the bending modulus ( $k_c$ ).

## Zeta-potential measurements

An SOPC/chloroform solution containing  $\sim 2.5$  mg of SOPC lipids was dried under vacuum for at least 2 h to completely evaporate chloroform. The lipid film was rehydrated with  $\sim 4$  ml of ultra-pure water at various pH values, and incubated at room temperature under nitrogen gas for at least 30 min and then extruded using the Mini-extruder with 100 nm polycarbonate filters (protocol of Avanti Polar Lipids) to ensure the formation of large unilamellar vesicles (LUVs)  $\sim 100$  nm in diameter. The electrophoretic mobility measurements of SOPC LUVs exposed to solutions with different pH values were obtained using the Zeta PALS  $\zeta$ -potential analyzer (Brookhaven Instrument, Holtsville, NY). The  $\zeta$ -potential was calculated from the mobility measurements automatically by the instrument utilizing the Smoluchowski equation (62).

## Dipole potential measurements

The spectral shifts of the potentiometric styryl probe, di-8 ANEPPS, were utilized to examine changes in dipole potential of membranes exposed to solutions with different pH values. The method follows that of Clarke and Lüpfer (51) and Xu and Loew (56). The LUVs composed of SOPC were synthesized as described above. Approximately  $3.5 \mu\text{l}$  of  $1 \text{ mg/ml}$  di-8 ANEPPS (in ethanol) was added to the LUV solution to achieve a lipid/probe ratio of  $\sim 400:1$ . The mixture was incubated under nitrogen gas. Spectral measurements were performed using a SpectraMax M2 spectrophotometer (Molecular Devices, Sunnyvale, CA). The emission wavelength was set at 670 nm and the excitation spectra between 400 nm and 550 nm were recorded (51,57). The ratio ( $F_{420/520}$ ) of fluorescence intensities at 420 nm and 520 nm of the excitation spectrum was used to calculate the dipole potential using the relationship (51,57):

$$\Psi_{\text{dipole}} = (F_{420/520} - 0.4)/5.4 \times 10^{-3}. \quad (4)$$

## Laurdan generalized polarization measurements

The bilayer phase behavior was monitored with the fluorescent probe Laurdan, following the techniques of Parassis et al. (63,64) and Bagatolli et al. (65–67). An appropriate amount of SOPC in chloroform was mixed with Laurdan (in ethanol) to achieve a lipid/probe ratio of  $\sim 300:1$ . The LUVs were formed as described above. The emission spectra between 400 nm and 500 nm were obtained at a fixed excitation wavelength chosen between 320 nm and 410 nm (66). Generalized polarization ( $GP_{\text{ex}}$ ) was then obtained by

$$GP_{\text{ex}} = \frac{I_{440} - I_{490}}{I_{440} + I_{490}}, \quad (5)$$

where  $I_{440}$  and  $I_{490}$  are fluorescent intensities detected at emission wavelength of 440 and 490 nm, respectively. The pattern of the  $GP_{\text{ex}}$  plot as a function of excitation wavelengths was utilized to indicate the bilayer phase behavior. As demonstrated previously, the GP spectra for a PC lipid tilts downward above the  $T_m$ , tilts upward near  $T_m$ , and is unaffected by the excitation wavelength below the main phase transition temperature (64).

## EXPERIMENTAL RESULTS

### Effect of pH on apparent area compressibility

The effect of pH on the apparent compressibility modulus of the membrane was first determined. All the  $\tau$  versus  $\alpha_{\text{app}}$  plots show a linear behavior in the high-tension domain ( $>0.5 \text{ mN/m}$ ), illustrating that the membrane behaved as linear elastic material in both acidic and basic environments.

Table 1 shows that  $K_{\text{app}}$  of the SOPC membrane was not affected by changes in solution pH until pH 2 ( $P < 0.05$ , all data were compared to the measurements conducted at pH 6.5 with no added ions and reported in our previous article (34)). At pH 2,  $K_{\text{app}}$  decreased to  $\sim 135 \text{ mN/m}$ , a  $\sim 35\%$  reduction compared to the  $K_{\text{app}}$  value of  $\sim 211 \text{ mN/m}$  at pH 6.5. This decrease in  $K_{\text{app}}$  indicates a weakening of the SOPC membrane. The change in lipid packing was also observed optically: many vesicles suspended in solution at pH 2 showed a half-moon shape, in which a portion of the membrane became linear and lost its curvature—an indication of phase separation (Fig. 2). In addition, aspiration on the half-moon-shaped vesicles showed that these vesicles were able to maintain the half-moon shape, indicating that externally applied pressure could not eliminate the phase separation.

### Bending rigidity ( $k_c$ ) and elastic area compressibility modulus ( $K_A$ )

The effect of pH on bending stiffness is shown in Table 1. The  $k_c$  of SOPC increased (with the student's  $t$ -test  $P < 0.05$ ) at both pH 4 ( $\sim 1.2 \times 10^{-19} \text{ J}$ ) and pH 9 ( $\sim 1.3 \times 10^{-19} \text{ J}$ ) and remained unchanged at pH 2 ( $\sim 0.87 \times 10^{-19} \text{ J}$ ) when compared to the  $k_c$  value of  $\sim 0.9 \times 10^{-19} \text{ J}$  at pH 6.5 (34), which agrees with earlier measurements for SOPC (32,38). The data was then subjected to an Analysis of Variance (ANOVA) test to assess the statistical significance of the pH effect on  $k_c$ . The ANOVA test supports the hypothesis that pH has an effect on SOPC bending stiffness ( $F = 4.8$  and  $P = 0.0024$ ). When  $k_c$  data for both pH 4 and pH 9 were removed, the ANOVA indicates that the rest of the pH values do not affect  $k_c$  ( $F = 0.47$  and  $P = 0.63$ ).

As mentioned above, the observed changes in  $K_{\text{app}}$  could actually reflect alterations in  $k_c$ . Therefore, the actual elastic

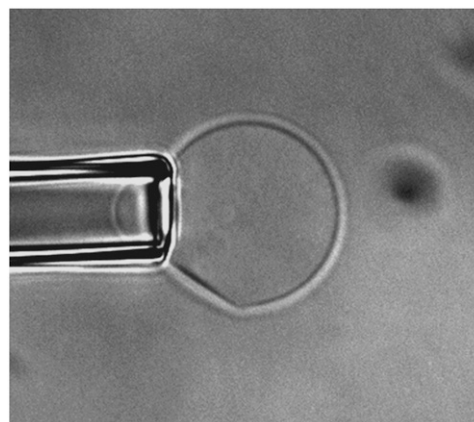


FIGURE 2 Half-moon-shaped vesicle aspirated into a micropipette at pH 2. The vesicle was held at least  $50 \mu\text{m}$  above the bottom surface of the chamber. A portion of the membrane became flat and lost its curvature, an indication of phase separation.

**TABLE 1** Effect of pH on membrane mechanical properties

pH	$k_c (\times 10^{-19} \text{ J})$	$K_{app} (\text{mN/m})$	$K_A (\text{mN/m})$	$k_{c-el} (\times 10^{-19} \text{ J})$
2	$0.87 \pm 0.2 (8)$	$135 \pm 49 (8)$	$166 \pm 65 (7)^*$	0.05
3	$0.98 \pm 0.34 (10)$	$205 \pm 27 (10)$	$257 \pm 48 (10)$	0.19
4	$1.22 \pm 0.36 (13)^*$	$205 \pm 41 (12)$	$246 \pm 56 (12)$	0.31
6.5	$0.90 \pm 0.15 (10)^\dagger$	$211 \pm 23 (17)^\dagger$	$247 \pm 32 (7)^\dagger$	0.11
9	$1.33 \pm 0.33 (12)^*$	$190 \pm 48 (10)$	$217 \pm 54 (10)$	0.53
10 mM NaCl at pH 4	$0.82 \pm 0.26 (11)$			

Values are shown as mean  $\pm$  SD. The numbers in parentheses represent the number of vesicles used during experiments.

\*Indicates values are statistically different from control (pH 6.5), as determined by a Student's *t*-test results obtained at 95% confidence. The ANOVA test supports the hypothesis that pH has an effect on SOPC bending stiffness ( $F = 4.8$  and  $P = 0.0024$ ) and on  $K_A$  at pH 2 ( $F = 4.18$  and  $P = 0.006$ ).

<sup>†</sup>Data obtained from our previous investigation (34).

area compressibility modulus ( $K_A$ ) is a more appropriate way to indicate changes in elasticity (32,34). When the area dilation caused by smoothing of the thermal undulations was removed, the  $K_A$  of SOPC at pH 2 was found to decrease to  $\sim 166$  mN/m from the control value of  $\sim 246$  mN/m previously determined at pH 6.5 (34). Table 1 shows that  $K_A$  is only affected at pH 2 (Student's *t*-test  $P < 0.05$ ). To further assess the statistical significance of pH effect on  $K_A$ , the ANOVA test was performed. The results support the hypothesis that pH 2 has an effect on  $K_A$  ( $F = 4.16$  and  $P = 0.006$  with all values of pH;  $F = 1.15$  and  $P = 0.34$  without pH 2).

### Effect of pH on electrophoretic mobility and $\zeta$ -potential

As solution pH varies, different concentrations of protons/hydroxide act as counterions to neutralize either phosphate or choline groups on PC lipids, thus potentially altering the surface charge (42–44,68,69). Fig. 3 shows that solution pH has significant effects on the surface charge of SOPC vesicles. At pH 2 and 3, SOPC vesicles have a positive  $\zeta$ -potential, indicating extensive association of protons at the

membrane surface. This agrees with other investigations demonstrating that phospholipids carry a positive  $\zeta$ -potential at low pHs (69). At pH 4, the  $\zeta$ -potential is nearly zero ( $\sim 3.5$  mV) and the LUVs showed low mobility, in agreement with other investigations demonstrating that the isoelectric point of PC lipids is  $\sim$ pH 4 (24–26,69). At the near neutral pH of 6.5, the  $\zeta$ -potential is clearly negative ( $\sim -21$  mV), in agreement with many investigations which have pointed out that PC is negatively charged between  $-10$  mV and  $-30$  mV at neutral pH (42–44,68,69). Silvander et al. (42) have utilized a surface probe, 4-heptadecyl-7-hydroxycoumarin, to titrate egg PC at low ionic strength and found anionic groups on PC at neutral pH. At pH 9, the  $\zeta$ -potential is also negative ( $\sim -20$  mV), indicating the binding of hydroxide ions with PC headgroups. The observed pattern of change in  $\zeta$ -potential as a function of solution pH also agrees with the theoretical predictions of Figaszewski and colleagues, who suggested that a form of PC bound with protons mainly exists at extremely low pHs, that pH 4 is the isoelectric point of PC lipids, and that PC lipids associated with hydroxide ions are the predominant form with pH above 4 (24–26).

### Effect of pH on dipole potential

Ions in the solution can also partition into PC membranes to affect the internal electrical properties. To examine possible changes in dipole potential caused by changing pH, we measured the dipole potential according to the method of Clarke (51,57) and Xu and Lowe (56). The excitation spectra of di-8 ANEPPS incorporated into SOPC LUVs at different solution pHs were obtained. The ratios ( $F_{420/520}$ ) in Table 2 indicate values between 1.5 and 1.6, in relative agreement with Clarke and Lüpfer (51) who reported the ratio for 18:0/18:1 PC is 1.424. Our results indicate that  $F_{420/520}$  changes significantly as a function of solution pH (Table 2). When compared with data at pH 9, we found that  $F_{420/520}$  increased as pH decreased. We did not test the dipole potential at pH 2 because the  $pK_a$  of di-8 ANEPPS is  $\sim 1.8$  (51), which would complicate data interpretation.

We estimated the dipole potential of SOPC membranes at different pH values (see Table 2). The  $\Psi_d$  values obtained

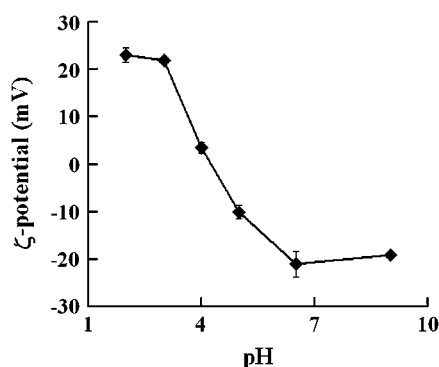


**FIGURE 3** The  $\zeta$ -potential, as calculated from electrophoretic mobility data, plotted as a function of solution pH. The values are shown as mean  $\pm$  SE. As shown, PC vesicles are positively charged at pH 2 and 3, near neutral at pH 4, and negatively charged at both pH 6.5 and 9.

**TABLE 2** Effect of pH on membrane dipole potential

pH	F (di-8 ANEPPS)	$\Psi_d$ (mV)
2	N/A	N/A
3	1.5801 $\pm$ 0.0102*	221.9 $\pm$ 9.4*
4	1.6027 $\pm$ 0.0330*	222.7 $\pm$ 9.8*
6.5	1.5635 $\pm$ 0.0215*	215.5 $\pm$ 6.2*
9	1.5084 $\pm$ 0.0381	205.3 $\pm$ 11

Values are shown as mean  $\pm$  SD. Experiments were repeated at least three times.

\*Indicates values are statistically different from pH 9, as determined by a Student's *t*-test at 95% confidence. The ANOVA test supports the hypothesis that pH has an effect on SOPC dipole potential ( $F = 11.2$  and  $P = 8.9 \times 10^{-6}$ ).

were  $\sim 200$ – $220$  mV, within the range of those of PC bilayers obtained by Clarke and colleagues (51,57,58). As shown, the SOPC dipole potential increased as pH decreased from 9 (with the student's *t*-test  $P < 0.05$  between pH 9 and other pHs, and ANOVA test  $F = 11.25$  and  $P = 8.9 \times 10^{-6}$ ).

### Gel-phase characteristics at pH 2

A phase-sensitive fluorescence probe, Laurdan, was utilized to examine possible SOPC gel-phase characteristics at pH 2. The emission generalized polarization ( $GP_{ex}$ ) spectra as a function of excitation wavelength can be utilized to indicate phase behavior below, near and above the main phase transition temperatures ( $T_m$ ) (66). As indicated by Bagatolli and Gratton (2000), the GP spectra for a PC lipid should tilt downward above the  $T_m$ , tilt upward near  $T_m$ , and become unaffected by the excitation wavelength below the main phase transition temperature (66). The excitation GP spectra for SOPC at pH 6.5 and pH 2 were examined between 400 nm and 500 nm. In Fig. 4, the downward tilting of the GP spectrum for SOPC at pH 6.5 clearly indicates that SOPC bilayer was in the liquid phase at 23°C. The first portion of the GP spectrum for SOPC at pH 2 is almost independent of the excitation wavelength and the later portion displays an upward tilt, both of which indicate that the LUVs composed of SOPC possess gel phase characteristics at pH 2. Furthermore, the positive GP values at pH 2 suggest that the fluorescence intensities obtained at 440 nm (gel phase maxima) is always higher than that obtained at 490 nm (liquid phase maxima), also indicating that the SOPC membrane has gel phase characteristics at pH 2. This also agrees with findings by Eibl and colleagues who have shown that low acidic pH values ( $<3$ ) shift the main phase transition temperatures of PC lipids to higher temperatures (6–8).

### DISCUSSION

Our  $k_c$ ,  $\zeta$ -potential, and  $\Psi_d$  measurements indicate that solution pH has significant effects on both mechanical and electrical properties of PC membranes. An immediate

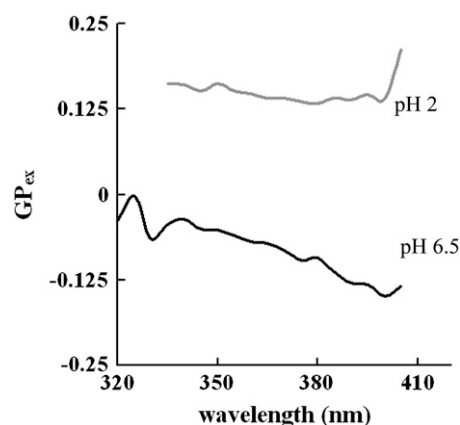


**FIGURE 4** The excitation GP spectra of SOPC LUVs with Laurdan at pH 6.5 (bottom) and pH 2 (top) at room temperature. The GP spectrum at pH 6.5 shows a downward tilt, indicating a liquid phase. The first portion of the GP spectrum for SOPC at pH 2 is almost independent of the excitation wavelength and the later portion displays an upward tilt, both indicating gel phase characteristics at pH 2. The positive GP values at pH 2 also suggest that the fluorescence intensities obtained at 440 nm (gel phase maxima) is always higher than that obtained at 490 nm (liquid phase maxima), indicating gel phase characteristics at pH 2.

concern is whether these changes are caused by changes in the titration state of PC functional groups. However, none of the functional groups has a  $pK_a$  within the range of pH 2–9: the  $pK_a$  is  $<2$  for phosphate (70),  $\sim 11$  for choline (70), and  $\sim -25$  for the ester carbonyl (71). Thus, pH effects observed in this investigation most likely result from other physical interactions, such as counterion binding and partitioning into the membrane.

The  $\zeta$ -potential measurements indicate that protons and hydroxide ions act as counterions and alter the external electrostatic environment of the membrane. The measured spectral shifts in the response of di-8 ANEPPS point to an effect of pH on the internal electrostatic environment of the membrane. In an attempt to explain the origin of these pH effects on membrane electrostatics and mechanics, we discuss our measurements in light of theoretical models, paying particular attention to the observed correlation between  $k_c$  and the electrical properties of the membrane.

### Effects of pH on membrane interfacial electrostatics and bending stiffness

The membrane bending stiffness contains both electrostatic and mechanical components (46,47). The lack of direct correlation between our measured  $k_c$  and the change in  $H^+/OH^-$  concentrations suggests that the bending stiffness is unlikely to be influenced by  $H^+/OH^-$  partitioning into the bilayer and directly changing the mechanical packing of the lipids, as expected from the small size of these ions. Thus, we hypothesize that changes in interfacial electrostatics plays the

major role in the observed effects of pH on the overall membrane bending stiffness. Electrolytes can not only alter the Debye length, but also potentially change the membrane surface charge and the charge density by acting as counterions and binding to lipids. Many investigators have demonstrated that the electrical properties of even zwitterionic PC headgroups are affected by counterion binding (43–45,62, 72), which changes the surface charge and the charge density of membranes. The relationship between membrane surface charge and membrane mechanical properties is an unresolved biophysical problem. The membrane bending stiffness has been theoretically predicted to have an intricate relationship with membrane interfacial electrical properties (46–50). Utilizing Poisson-Boltzmann theory, Winterhalter and Helfrich (47) have constructed a model that predicts that the electrostatic contributions from both solution Debye length and membrane surface charge density can affect bending stiffness (47). In this model (47), the electrostatic portion of the bending stiffness,  $k_{c-el}$ , can be expressed as

$$k_{c-el} = \left( \frac{2k_B T}{e} \right)^2 \frac{\epsilon_w}{\kappa} \frac{(A-1)}{A(A+1)} \left[ (A+2) - 2 \frac{B}{A-B} \right], \quad (6)$$

where  $A = \{1 + [\sigma e / (2\epsilon_w k_B T \kappa)]^2\}^{1/2}$ ,  $B = (\epsilon_i / \epsilon_w)(1/\kappa h)$ ,  $\sigma$  is the membrane surface charge density,  $\kappa$  is  $1/\text{Debye length}$ ,  $\epsilon_w$  is the dielectric constant of water,  $\epsilon_i$  is the dielectric constant of membranes,  $e$  is the elementary charge, and  $h$  is the thickness of the membrane. This model predicts that an increase in  $\sigma$  will increase  $k_{c-el}$  at a fixed Debye length (47). Likewise, alterations in the Debye length will shift the  $k_{c-el}$  versus  $\sigma$ -curve. A particular prediction of this model is that  $k_{c-el}$  reaches a plateau when a membrane with a high surface charge density is exposed to a solution with high ionic strength (47). To estimate  $k_{c-el}$ , we nominally chose the value of  $k_c$  we measured at pH 3, where  $1/\kappa = \sim 10$  nm and surface charge is high (suggested by our  $\zeta$ -potential measurements). Under these conditions,  $k_{c-el}$  should be at a plateau value, which Winterhalter and Helfrich (47) predict to be  $\sim 0.2 \times 10^{-19}$  J. Subtracting this from our data at pH 3, we estimate that the mechanical component of the bending stiffness,  $k_{c-m}$ , is  $\sim 0.78 \times 10^{-19}$  J. Under the hypothesis that the measured alteration in the overall bending stiffness as a function of pH results from electrostatic effects, we can assume that  $k_{c-m}$  remains fixed throughout the tested pH range, and any difference between our measured  $k_c$  and  $\sim 0.78 \times 10^{-19}$  J reflect the electrostatic contributions to  $k_c$  at that specific pH (listed in Table 1). With a view to illustrating trends, we plotted our measured  $k_{c-el}$  versus  $\ln 1/\kappa$  (Fig. 5, *open circles*) and utilized Eq. 6 to estimate the membrane surface charge density,  $\sigma_{est}$ , at different pH values (Fig. 5, *solid and dashed lines*). Fig. 5 demonstrates that, with a fixed surface charge density, an increase in the Debye length will cause an increase in  $k_{c-el}$  and changes in  $\sigma_{est}$  shift the  $k_{c-el}$  versus  $\ln 1/\kappa$  curve, qualitatively in agreement with the prediction of Winterhalter and Helfrich (47).

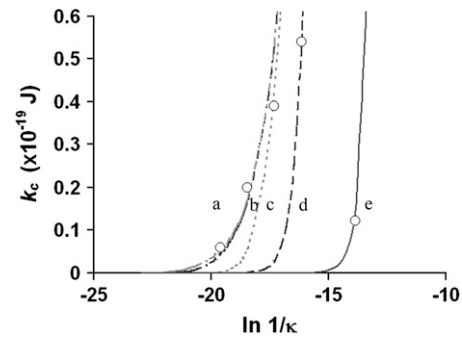


FIGURE 5 Plot of measured  $k_{c-el}$  against  $\ln 1/\kappa$  (*open circles*). The membrane surface charge density,  $\sigma_{est}$ , was estimated by fitting Eq. 6 (*solid and dashed lines*) to the experimental data. In the plot, *a* is pH 2 with  $\sigma_{est} = 0.1$  C/m<sup>2</sup>, *b* is pH 3 with  $\sigma_{est} = 0.03$  C/m<sup>2</sup>, *c* is pH 4 with  $\sigma_{est} = 0.003$  C/m<sup>2</sup>, *d* is pH 9 with  $\sigma_{est} = 3.3 \times 10^{-4}$  C/m<sup>2</sup>, and *e* is pH 6.5 with  $\sigma_{est} = 6 \times 10^{-6}$  C/m<sup>2</sup>.

The membrane surface charge density can also be estimated from our  $\zeta$ -potential measurements (73,74). A simple way to relate  $\zeta$ -potential to the surface potential is by the approximation  $\Psi_s = \zeta \exp(-\kappa x)$ , where  $\Psi_s$  is the surface potential and  $x$  is the distance from the shear plane (the boundary between the fixed ion layer and the diffuse ion layer) to the interface, estimated to be  $\sim 0.2$  nm (73,74). The surface potential can be utilized to approximate the surface charge density,  $\sigma_{cal}$  (69,75)

$$\sigma_{cal}^2 = 2\epsilon_w \epsilon_0 RT \sum_{i=1}^n C_i \left[ \exp\left(\frac{-ZF\Psi_s}{RT}\right) - 1 \right], \quad (7)$$

where  $C_i$  is the aqueous ion concentration,  $Z$  is the valence of the ion,  $F$  is the Faraday constant, and  $R$  is the gas constant. Using the value of surface charge density estimated from our measured  $k_c$  and Eq. 6,  $\sigma_{est}$ , and the value of surface charge density calculated from our independently measured  $\zeta$ -potential data,  $\sigma_{cal}$ , we plotted  $\ln(\sigma_{est})$  versus  $\ln(\sigma_{cal})$  (Fig. 6). The correlation in Fig. 6 indicates that changes in the membrane surface charge density caused by alterations in solution pH correlate with modifications in the overall bending stiffness. Note that the actual values of  $\sigma_{cal}$  do not match those of  $\sigma_{est}$  exactly, since both models utilized in calculations are approximations. However, the qualitative trend is important in the comparison. The good correlation in Fig. 6 supports the hypothesis that electrostatics plays a major role in the pH effect on the overall bending stiffness of SOPC membranes.

Furthermore, Fig. 5 demonstrates that both the membrane surface charge density and the solution Debye length contribute to the changes in the bending stiffness. At the extreme pH values of 2 and 3, high concentrations of protons (10 mM at pH 2) in the solution result in more ions available to bind with PC lipids when compared to pH 6.5, thus increasing the membrane surface charge (as supported by our  $\zeta$ -potential

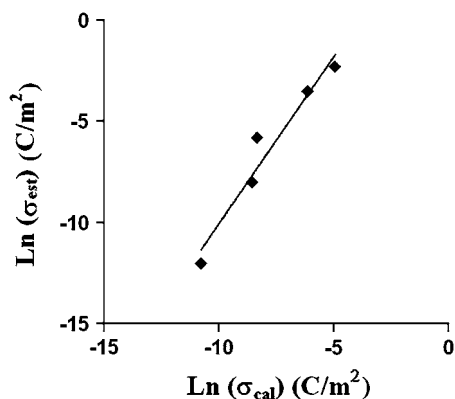


FIGURE 6 The correlation between the estimated PC membrane surface charge density,  $\sigma_{\text{est}}$ , and membrane surface charge density calculated from the  $\zeta$ -potential data,  $\sigma_{\text{cal}}$ . The linear correlation ( $R^2 = 0.9466$ ) between  $\sigma_{\text{est}}$  and  $\sigma_{\text{cal}}$  indicates that electrostatics play an important role in influencing membrane mechanical properties.

measurements in Fig. 3). This is expected to increase the bending stiffness. However, high concentrations of ions also increase  $\kappa$  (the inverse Debye length), which mainly negatively influences the bending stiffness (46,47). Both the model and data support the hypothesis that the sharp decreases in Debye length at pH 2 and 3 out-compete the increase of the surface charge density at the interface, yielding a small  $k_{\text{c-el}}$  and a negligible change in the overall bending stiffness. At moderate pH values of 4 and 9, the change in surface charge density apparently out-competes the decrease in Debye length, thus increasing the electrical component of the bending stiffness and yielding a larger overall bending stiffness.

To test this hypothesis, we measured  $k_c$  of SOPC vesicles exposed to a pH 4 solution containing 10 mM NaCl, which gives a shorter Debye length than the original pH 4 solution. As predicted by Winterhalter and Helfrich (47), a decrease in  $1/\kappa$  to  $<10$  nm would yield a  $k_{\text{c-el}}$  too small to be detected by experiments. Our measured  $k_c$  at pH 4 with 10 mM NaCl ( $\sim 0.82 \times 10^{-19}$  J) demonstrates that 10 mM NaCl diminished the effect of the original pH 4 solution on the  $k_c$  of SOPC ( $\sim 1.2 \times 10^{-19}$  J). The evidence that low concentrations of inorganic monovalent salts do not affect  $K_{\text{app}}$  (35), which is also influenced by  $k_c$  (32), suggests that 10 mM NaCl does not directly affect membrane-bending stiffness. Thus, we hypothesize that the decrease in overall bending stiffness at pH 4 with the addition of 10 mM NaCl results from the shortening of Debye length when compared to the original pH 4 solution.

Song and Waugh (76) previously investigated the effect of membrane surface charge on membrane bending stiffness using tether-formation experiments. They found no statistically significant difference in the bending stiffness between 100% SOPC and SOPC vesicles containing 14% palmitoyl oleoyl phosphatidylserine (76), which should increase the membrane surface charge density and increase  $k_{\text{c-el}}$ . The reason for this discrepancy is not clear. One possible explanation

could be that it may be energetically unfavorable for the charged PS to enter the highly curved tether. Another possibility is that the packing in mixed PC/PS membranes could reduce  $k_{\text{c-m}}$  and offset the surface charge density increase.

### Effect of pH on membrane dipole potential

We have demonstrated above that solution pH affects both membrane mechanical and interfacial electrical properties and that alterations in membrane surface charge density and the Debye length can account for the experimentally measured changes in the membrane bending stiffness. This raises the question whether pH also affects the internal electrostatic properties of the membrane and whether there is a correlation between intramembrane electrical properties and mechanics. To investigate this, we measured changes in the intramembrane (dipole) potential as a function of solution pH (Table 2). The data in Table 2 are most clearly displayed by plotting dipole potential versus pOH, which demonstrates a linear correlation (Fig. 7). If the affinity of proton and hydroxide ions for membranes is the same, there should be a symmetric change in dipole potential as a function of pH centered at pH 7. The linear correlation observed in Fig. 7 suggests that either protons or hydroxide ions play a dominant role in affecting  $\Psi_d$ . Clarke and Lüpfer (51) established that the effectiveness of an ion in reducing the membrane dipole potential depends on the free energies of hydration,  $\Delta G_{\text{hyd}}$ , of the ion as well as whether the ion is positively or negatively charged. It was found that hydrophobic anions and hydrophilic cations tend to be more effective at altering the membrane dipole potential (51). Theoretical calculations estimate that  $\Delta G_{\text{hyd}}$  for protons and hydroxide ions is  $\sim -260$  kJ/mol (77). This value indicates that these ions are relatively hydrophobic compared to other ions, such as  $\text{Mg}^{2+}$  with  $\sim -2000$  kJ/mol and  $\text{SO}_4^{2-}$  with  $\sim -1150$  kJ/mol (51). Thus, it is likely that the relatively hydrophobic hydroxide ion is more effective at interacting with lipids than an equally hydrophobic proton. Since the  $\zeta$ -potential is mainly a measure of the surface charge, a negative  $\zeta$ -potential at pH 6.5 (Fig. 3) also points to the possibility that hydroxide ions associate with PC lipids more favorably than protons. Even with a slight excess of protons in the solution at pH 6.5, more hydroxide ions potentially associate with PC, yielding a negatively charged membrane. This also agrees with the studies of Ninham and colleagues (78,79), who suggest that the affinity of a particular ion for membranes depends upon the polarizability of the ion, or the ionic dispersion coefficient. A much more polarizable hydroxide ion should interact with membranes more favorably than a proton, which is not polarizable (78,79). In addition, both inorganic anions and cations decrease the dipole potential (51). The inability of acidic pHs, even at pH 3, to decrease the SOPC dipole potential also suggests that it is unlikely that protons are the cause of any changes



in the dipole potential. Therefore, the partitioning of the anionic hydroxide ions potentially decreases the PC dipole potential, and a decrease in hydroxide concentration as the solution pH decreases is consistent with increases in the dipole potential.

The fact that the hydrophobic cations do not affect the dipole potential (51) indicates that the effect of inorganic ions on the membrane dipole potential is potentially dominated by electrostatic interactions. As the membrane dipole potential is positive in the bilayer core, the partitioning of anionic hydroxide ions would diminish the interior positive characteristics and decrease the dipole potential, as supported by our data (Table 2). At acidic pH values, the decreasing hydroxide concentration corresponds to larger dipole potentials. At pH 9, the dipole potential is associated with the highest  $k_c$ , while the increase in dipole potential at acidic pHs corresponds to a lower  $k_c$  at pH 3 and pH 6.5 and an unchanged  $k_c$  at pH 4 when compared with  $k_c$  at pH 9. Because the di-8 ANEPPS spectral shift is a reflection of the membrane internal properties (56), the lack of direct correlation between bending stiffness and dipole potential further indicates that interfacial electrostatic contributions play a main role in the pH effect on PC bending stiffness.

A final interesting observation on the  $\Psi_d$  measurements is that the concentrations of hydroxide ions needed to affect PC membrane dipole potential are much less than those of Hofmeister ions. The maximal amount of hydroxide ions tested was 10  $\mu\text{M}$  (at pH 9), while concentrations of Hofmeister ions are 500 mM in the study of Clarke and Lüpfer (51). This suggests that hydroxide ions are much more effective in terms of their ability to affect membrane dipole potential. It has been established that proton/hydroxide permeability is as much as nine orders-of-magnitude faster than other monovalent Hofmeister ions, indicating more favorable interactions between protons/hydroxide and membranes (80–82).

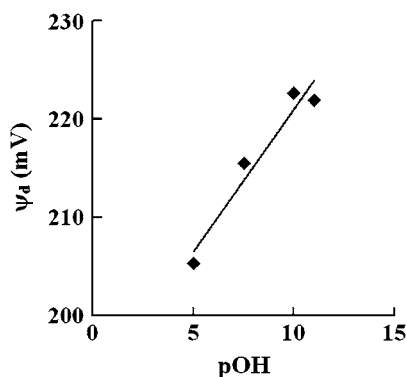


FIGURE 7 The SOPC dipole potential was plotted against pOH, demonstrating that the dipole potential increases as solution pH decreases ( $R^2 = 0.9403$ ).

## Gel-phase characteristics at pH 2

Eibl and colleagues have shown that low acidic pH ( $\text{pH} < 3$ ) increases the main phase transition temperatures ( $T_m$ ) of C-14/16 lecithin lipids by as much as  $\sim 10^\circ\text{C}$  while higher pH values had no detectable effects on  $T_m$  (6–8). This suggests that PC lipid lateral packing is not changed in this pH range ( $\text{pH} > 3$ ), which agrees with our finding that  $K_A$  was unaffected by changes in pH between 3 and 9. However, our data show a large drop in  $K_A$  by  $\sim 30\%$  at pH 2, indicating a dramatic disruption in membrane cohesiveness. This observed decrease in  $K_A$  is not caused by changes in the chemical composition of the SOPC membrane, as shown by thin layer chromatography experiments (data not shown). Theoretical (83,84) and experimental (85–87) studies demonstrated that membrane stability is reduced within the phase transition region. This is attributed to the presence of domains, which disrupt membrane continuity and weaken the entire bilayer structure. In addition to our mechanical data, we visually observed gel-phase characteristics in SOPC membranes at pH 2 (Fig. 2). The uncharacteristically wide spread of our  $K_A$  data at pH 2 also points to the possibility that multiple phases could exist at pH 2. To further confirm this possibility, we utilized Laurdan to examine the phase behavior of SOPC LUVs at pH 2. We found that the excitation GP spectrum at pH 2 indicates the presence of gel phase characteristics (Fig. 4). Furthermore, although the GUVs we used were single-component system (100% SOPC) which should have a sharp transition, it has been suggested that giant vesicles have a broader transition because of lack of cooperative unit size in the GUVs as compared to LUVs, which are commonly used to determine  $T_m$  (67). Thus, an increase in the  $T_m$  and a potential broadening of the transition region in GUVs may be the mechanisms that explain the observed gel-phase characteristics in LUVs and GUVs at pH 2 and lower bilayer elasticity.

## CONCLUSIONS

The solution pH is a crucial factor in ensuring normal cellular function. We have systematically characterized the effect of pH on the mechanical and electrical properties of SOPC membranes. Mechanical, interfacial electrical, and internal electrical measurements combine to support the view that changes in membrane bending stiffness result from alterations in interfacial electrostatics. Specifically, increases in  $k_c$  at pH 4 and pH 9 reflect changes in membrane surface charge density and Debye length. Although the membrane dipole potential increases as solution pH decreases, this likely originates from hydroxide ion interactions with membranes and does not correlate with  $k_c$ . The elastic compressibility of membranes is insensitive to pH, except for a decrease at pH 2, which is attributed to the presence of gel-phase characteristics. Hence, the alteration of solution pH is a straightforward method to study the relationship between mechanical

and electrical properties of membranes. These results indicate that membrane electrical properties and mechanical properties are interconnected, supporting the emerging paradigm of the membrane as an electro-mechanical structure.

We thank Drs. Huey W. Huang, Jane Grande-Allen, and Michael S. Wong for equipment access. We are grateful to Drs. Nathan Baker and Kevin Mackenzie for insightful discussions and for critiquing a draft of this manuscript.

This study was supported in part by grants from the State of Texas Technology Development and Transfer Program and a National Science Foundation Career Award (BES 0449379).

## REFERENCES

- Chernomordik, L. V., E. Leikina, V. Frolov, P. Bronk, and J. Zimmerberg. 1997. An early stage of membrane fusion mediated by the low pH conformation of influenza hemagglutinin depends upon membrane lipids. *J. Cell Biol.* 136:81–93.
- Redfern, D. A., and A. Gericke. 2004. Domain formation in phosphatidylinositol monophosphate/phosphatidylcholine mixed vesicles. *Biophys. J.* 86:2980–2992.
- Redfern, D. A., and A. Gericke. 2005. pH-dependent domain formation in phosphatidylserine polyphosphate/phosphatidylcholine mixed vesicles. *J. Lipid Res.* 46:504–515.
- Carrozzino, J. M., and M. G. Khaledi. 2005. pH effects on drug interactions with lipid bilayers by liposome electrokinetic chromatography. *J. Chromatogr. A.* 1079:307–316.
- Cevc, G., A. Watts, and D. Marsh. 1981. Titration of the phase transition of phosphatidylserine bilayer membranes. Effects of pH, surface electrostatics, ion binding, and head-group hydration. *Biochemistry.* 20:4955–4965.
- Eibl, H., and A. Blume. 1979. The influence of charge on phosphatidic acid bilayer membranes. *Biochim. Biophys. Acta.* 553:476–488.
- Trauble, H., and H. Eibl. 1974. Electrostatic effects on lipid phase transitions: membrane structure and ionic environment. *Proc. Natl. Acad. Sci. USA.* 71:214–219.
- Trauble, H., M. Teubner, P. Woolley, and H. Eibl. 1976. Electrostatic interactions at charged lipid membranes. I. Effects of pH and univalent cations on membrane structure. *Biophys. Chem.* 4:319–342.
- Stumpel, J., K. Harlos, and H. Eibl. 1980. Charge-induced pretransition in phosphatidylethanolamine multilayers. The occurrence of ripple structures. *Biochim. Biophys. Acta.* 599:464–472.
- Smith, B. D., and P. L. La Celle. 1979. Parallel decrease of erythrocyte membrane deformability and spectrin solubility at low pH. *Blood.* 53:15–18.
- Heuser, J. 1989. Changes in lysosome shape and distribution correlated with changes in cytoplasmic pH. *J. Cell Biol.* 108:855–864.
- Campbell, N. A., and J. B. Reece. 2002. *Biology*. Benjamin/Cummings, San Francisco, CA.
- Barreto, J., and L. M. Lichtenberger. 1992. Vesicle acidification driven by a millionfold proton gradient: a model for acid influx through gastric cell membranes. *Am. J. Physiol.* 262:G30–G34.
- Lichtenberger, L. M. 1987. Membranes and barriers: with a focus on the gastric mucosal barrier. *Clin. Invest. Med.* 10:181–188.
- Nylander-Koski, O., H. Mustonen, I. Vikholm, T. Kiviluoto, and E. Kivilaakso. 2001. HCl causes less intracellular acidification in *Necturus* gastric mucosa surface epithelial cells than other acids. *Am. J. Physiol. Gastrointest. Liver Physiol.* 281:G675–G680.
- Sulkowski, W. W., D. Pentak, K. Nowak, and A. Sulkowska. 2005. The influence of temperature, cholesterol content and pH on liposome stability. *J. Mol. Struct.* 744:737–747.
- Smaby, J. M., J. M. Muderhwa, and H. L. Brockman. 1994. Is lateral phase separation required for fatty acid to stimulate lipases in a phosphatidylcholine interface? *Biochemistry.* 33:1915–1922.
- Liu, H., R. Z. Lu, J. G. Turcotte, and R. H. Notter. 1994. Dynamic interfacial properties of surface-excess films of phospholipids and phosphonolipids analogs. *J. Colloid Interface Sci.* 167:378–390.
- Petiat, F., and S. Giasson. 2005. Study of pH-sensitive copolymer/phospholipid complexes using the Langmuir balance technique: effect of anchoring sequence and copolymer molecular weight. *Langmuir.* 21:7326–7334.
- Leonard, M. R., M. A. Bogle, M. C. Carey, and J. M. Donovan. 2000. Spread monomolecular films of monohydroxy bile acids and their salts: influence of hydroxyl position, bulk pH, and association with phosphatidylcholine. *Biochemistry.* 39:16064–16074.
- Furuike, S., V. G. Levadny, S. J. Li, and M. Yamazaki. 1999. Low pH induces an interdigitated gel to bilayer gel phase transition in dihexadecylphosphatidylcholine membrane. *Biophys. J.* 77:2015–2023.
- Harlos, K., J. Stumpel, and H. Eibl. 1979. Influence of pH on phosphatidic acid multilayers. A rippled structure at high pH values. *Biochim. Biophys. Acta.* 555:409–416.
- Blume, A., and H. Eibl. 1979. The influence of charge on bilayer membranes. Calorimetric investigations of phosphatidic acid bilayers. *Biochim. Biophys. Acta.* 558:13–21.
- Petelska, A. D., and Z. A. Figaszewski. 1998. Interfacial tension of two-component bilayer lipid membrane modeling of the cell membrane. *Bioelectrochem. Bioenerg.* 46:199–204.
- Petelska, A. D., and Z. A. Figaszewski. 2000. Effect of pH on the interfacial tension of lipid bilayer membrane. *Biophys. J.* 78: 812–817.
- Petelska, A. D., and Z. A. Figaszewski. 2002. Effect of pH on the interfacial tension of bilayer lipid membrane formed from phosphatidylcholine or phosphatidylserine. *Biochim. Biophys. Acta.* 1561: 135–146.
- Gennis, R. B. 1989. *Biomembrane Molecular Structure and Function*. C. R. Cantor, editor. Springer-Verlag, New York.
- Cevc, G., and D. Marsh. 1987. *Phospholipid Bilayers: Physical Principles and Models*. E. E. Bittar, editor. John Wiley & Sons, New York, NY.
- Israelachvili, J. N., D. J. Mitchell, and B. W. Ninham. 1976. Theory of self-assembly of hydrocarbon amphiphiles into micelles and bilayers. *J. Chem. Soc. Faraday Trans. II.* 72:1525–1568.
- Israelachvili, J. N., S. Marcelja, and R. G. Horn. 1980. Physical principles of membrane organization. *Q. Rev. Biophys.* 13:121–200.
- Evans, E. A., and R. Skalak. 1980. *Mechanics and Thermodynamics of Biomembranes*. CRC Press, Boca Raton, FL.
- Rawicz, W., K. C. Olbrich, T. McIntosh, D. Needham, and E. Evans. 2000. Effect of chain length and unsaturation on elasticity of lipid bilayers. *Biophys. J.* 79:328–339.
- Glassinger, E., A. C. Lee, and R. M. Raphael. 2005. Electromechanical effects on tether formation from lipid membranes: a theoretical analysis. *Phys. Rev. E Stat. Nonlin. Soft Matter Phys.* 72:041926.
- Zhou, Y., and R. M. Raphael. 2005. Effect of salicylate on the elasticity, bending stiffness, and strength of SOPC membranes. *Biophys. J.* 89:1789–1801.
- Shoemaker, S. D., and T. K. Vanderlick. 2002. Intramembrane electrostatic interactions destabilize lipid vesicles. *Biophys. J.* 83: 2007–2014.
- Needham, D., and R. S. Nunn. 1990. Elastic deformation and failure of lipid bilayer membranes containing cholesterol. *Biophys. J.* 58:997–1009.
- Needham, D., and D. V. Zhelev. 1995. Lysolipid exchange with lipid vesicle membranes. *Ann. Biomed. Eng.* 23:287–298.
- Ly, H. V., and M. L. Longo. 2004. The influence of short-chain alcohols on interfacial tension, mechanical properties, area/molecule, and permeability of fluid lipid bilayers. *Biophys. J.* 87:1013–1033.

39. Kwok, R., and E. Evans. 1981. Thermoelasticity of large lecithin bilayer vesicles. *Biophys. J.* 35:637–652.
40. Hung, V. L., D. E. Block, and M. L. Longo. 2002. Interfacial tension effect of ethanol on lipid bilayer rigidity, stability, and area/molecule: a micropipette aspiration approach. *Langmuir*. 18:8988–8995.
41. Evans, E. A., W. Rawicz, and A. Hoffmann. 1994. Lipid Bilayer Expansion and Mechanical Degradation in Solutions of Water-Soluble Bile Acids. A. Hoffmann, G. Baumgartner, and A. Stiehl, editors. San Diego, CA.
42. Silvander, M., P. Hansson, and K. Edwards. 2000. Liposomal surface potential and bilayer packing as affected by PEG-lipid inclusion. *Langmuir*. 16:3696–3702.
43. Tatulian, S. A. 1983. Effect of lipid phase transition on the binding of anions to dimyristoylphosphatidylcholine liposomes. *Biochim. Biophys. Acta*. 736:189–195.
44. Petrache, H. I., T. Zemb, L. Belloni, and V. A. Parsegian. 2006. Salt screening and specific ion adsorption determine neutral-lipid membrane interactions. *Proc. Natl. Acad. Sci. USA*. 103:7982–7987.
45. Petrache, H. I., S. Tristram-Nagle, D. Harries, N. Kucerka, J. F. Nagle, and V. A. Parsegian. 2006. Swelling of phospholipids by monovalent salt. *J. Lipid Res.* 47:302–309.
46. Winterhalter, M., and W. Helfrich. 1988. Effect of surface charge on the curvature elasticity membranes. *J. Phys. Chem.* 92:6865–6867.
47. Winterhalter, M., and W. Helfrich. 1992. Bending elasticity of electrical charged bilayers: coupled monolayers, neutral surfaces, and balancing stresses. *J. Phys. Chem.* 96:327–330.
48. Lekkerkerker, H. N. W. 1989. Contribution of the electric double layer to the curvature elasticity of charged amphiphilic monolayers. *Physica A*. 159:319–328.
49. Mitchell, D. J., and B. W. Ninham. 1989. Curvature elasticity of charged membranes. *Langmuir*. 5:1121–1123.
50. Duplantier, B., R. E. Goldstein, V. Romero-Rochn, and A. I. Pesci. 1990. Geometrical and topological aspects of electric double layers near curved surfaces. *Phys. Rev. Lett.* 65:508–511.
51. Clarke, R. J., and C. Lupfert. 1999. Influence of anions and cations on the dipole potential of phosphatidylcholine vesicles: a basis for the Hofmeister effect. *Biophys. J.* 76:2614–2624.
52. Brockman, H. 1994. Dipole potential of lipid membranes. *Chem. Phys. Lipids*. 73:57–79.
53. Clarke, R. J. 2001. The dipole potential of phospholipid membranes and methods for its detection. *Adv. Colloid Interface Sci.* 89–90:263–281.
54. Honig, B. H., W. L. Hubbell, and R. F. Flewelling. 1986. Electrostatic interactions in membranes and proteins. *Annu. Rev. Biophys. Biophys. Chem.* 15:163–193.
55. Franklin, J. C., and D. S. Cafiso. 1993. Internal electrostatic potentials in bilayers: measuring and controlling dipole potentials in lipid vesicles. *Biophys. J.* 65:289–299.
56. Xu, C., and L. M. Loew. 2003. The effect of asymmetric surface potentials on the intramembrane electric field measured with voltage-sensitive dyes. *Biophys. J.* 84:2768–2780.
57. Clarke, R. J. 1997. Effect of lipid structure on the dipole potential of phosphatidylcholine bilayers. *Biochim. Biophys. Acta*. 1327:269–278.
58. Starke-Peterkovic, T., N. Turner, M. F. Vitha, M. P. Waller, D. E. Hibbs, and R. J. Clarke. 2006. Cholesterol effect on the dipole potential of lipid membranes. *Biophys. J.* 90:4060–4070.
59. Angelova, M. J., S. Soleau, P. Melaeard, J. F. Faucon, and P. Bothorel. 1992. Preparation of giant vesicles by AC electric fields. kinetic and applications. *Prog. Colloid Polym. Sci.* 89:127–131.
60. Evans, E., V. Heinrich, F. Ludwig, and W. Rawicz. 2003. Dynamic tension spectroscopy and strength of biomembranes. *Biophys. J.* 85:2342–2350.
61. Evans, E., and W. Rawicz. 1990. Entropy-driven tension and bending elasticity in condensed-fluid membranes. *Phys. Rev. Lett.* 64:2094–2097.
62. McLaughlin, S. 1989. The electrostatic properties of membranes. *Annu. Rev. Biophys. Biophys. Chem.* 18:113–136.
63. Parasassi, T., E. de Felip, F. Lepore, and F. Conti. 1986. Calcium-induced phase separation in phospholipid bilayers. A fluorescence anisotropy study. *Cell. Mol. Biol.* 32:261–266.
64. Parasassi, T., G. De Stasio, A. d'Ubaldo, and E. Gratton. 1990. Phase fluctuation in phospholipid membranes revealed by Laurdan fluorescence. *Biophys. J.* 57:1179–1186.
65. Bagatolli, L. A., E. Gratton, and G. D. Fidelio. 1998. Water dynamics in glycosphingolipid aggregates studied by LAURDAN fluorescence. *Biophys. J.* 75:331–341.
66. Bagatolli, L. A., and E. Gratton. 2000. Two photon fluorescence microscopy of coexisting lipid domains in giant unilamellar vesicles of binary phospholipid mixtures. *Biophys. J.* 78:290–305.
67. Bagatolli, L. A., and E. Gratton. 1999. Two-photon fluorescence microscopy observation of shape changes at the phase transition in phospholipid giant unilamellar vesicles. *Biophys. J.* 77:2090–2101.
68. Smejtek, P., A. Blochel, and S. Wang. 1996. Hydrophobicity and adsorption of chlorophenolates to lipid membranes. *Chemosphere*. 33:177–201.
69. Kinraide, T. B., U. Yermiyahu, and G. Rytwo. 1998. Computation of surface electrical potentials of plant cell membranes. Correspondence to published  $\zeta$ -potentials from diverse plant sources. *Plant Physiol.* 118:505–512.
70. Tocanne, J. F., and J. Teissie. 1990. Ionization of phospholipids and phospholipid-supported interfacial lateral diffusion of protons in membrane model systems. *Biochim. Biophys. Acta*. 1031:111–142.
71. Loundon, G. M. 1995. Organic Chemistry. A. Scanlan-Rohrer, editor. Benjamin/Cummings, Redwood City, CA.
72. Heinz, W. F., and J. H. Hoh. 1999. Relative surface charge density mapping with the atomic force microscope. *Biophys. J.* 76:528–538.
73. Gilbert, D. L., and G. Ehrenstein. 1969. Effect of divalent cations on potassium conductance of squid axons: determination of surface charge. *Biophys. J.* 9:447–463.
74. Cole, K. S. 1969. Zeta potential and discrete versus uniform surface charges. *Biophys. J.* 9:465–469.
75. Lau, A., A. McLaughlin, and S. McLaughlin. 1981. The adsorption of divalent cations to phosphatidylglycerol bilayer membranes. *Biochim. Biophys. Acta*. 645:279–292.
76. Song, J., and R. Waugh. 1990. Bilayer membrane bending stiffness by tether formation from mixed PC-PS lipid vesicles. *J. Biomech. Eng.* 112:235–240.
77. Tawa, G. J., I. A. Topol, S. K. Burt, R. A. Calwell, and A. A. Rashin. 1998. Calculation of the aqueous solvation free energy of the proton. *J. Chem. Phys.* 109:4852–4863.
78. Bostrom, M., D. R. Williams, and B. W. Ninham. 2001. Specific ion effects: why DLVO theory fails for biology and colloid systems. *Phys. Rev. Lett.* 87:168103.
79. Bostrom, M., D. R. Williams, P. R. Stewart, and B. W. Ninham. 2003. Hofmeister effects in membrane biology: the role of ionic dispersion potentials. *Phys. Rev. E Stat. Nonlin. Soft Matter Phys.* 68:041902.
80. Nagle, J. F. 1987. Theory of passive proton conductance in lipid bilayers. *J. Bioenerg. Biomembr.* 19:413–426.
81. Nichols, J. W., and D. W. Deamer. 1980. Net proton-hydroxyl permeability of large unilamellar liposomes measured by an acid-base titration technique. *Proc. Natl. Acad. Sci. USA*. 77:2038–2042.
82. Nichols, J. W., M. W. Hill, A. D. Bangham, and D. W. Deamer. 1980. Measurement of net proton-hydroxyl permeability of large unilamellar liposomes with the fluorescent pH probe, 9-aminoacridine. *Biochim. Biophys. Acta*. 596:393–403.

83. Mouritsen, O. G., and M. J. Zuckermann. 1985. Softening of lipid bilayers. *Eur. Biophys. J.* 12:75–86.
84. Nagle, J. F., and H. L. Scott, Jr. 1978. Lateral compressibility of lipid mono- and bilayers. Theory of membrane permeability. *Biochim. Biophys. Acta.* 513:236–243.
85. Evans, E., and R. Kwok. 1982. Mechanical calorimetry of large dimyristoylphosphatidylcholine vesicles in the phase transition region. *Biochemistry.* 21:4874–4879.
86. Mills, J. K., and D. Needham. 2005. Lysolipid incorporation in dipalmitoylphosphatidylcholine bilayer membranes enhances the ion permeability and drug release rates at the membrane phase transition. *Biochim. Biophys. Acta.* 1716:77–96.
87. Papahadjopoulos, D., K. Jacobson, S. Nir, and T. Isac. 1973. Phase transitions in phospholipid vesicles. Fluorescence polarization and permeability measurements concerning the effect of temperature and cholesterol. *Biochim. Biophys. Acta.* 311:330–348.